SUPPLEMENTAL MATERIAL

Rashidian et al., https://doi.org/10.1084/jem.20161950

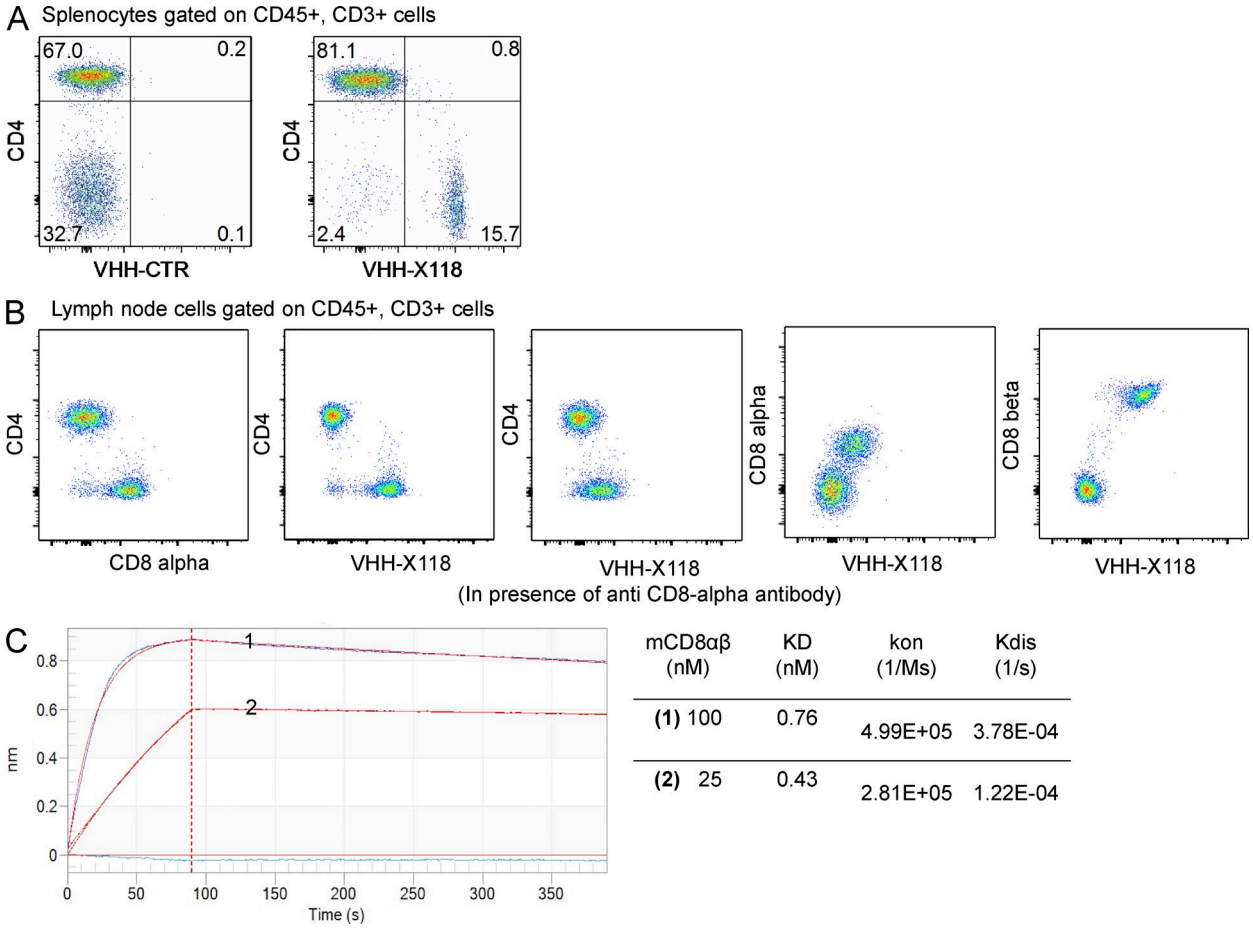


| mCD8αβ (nM) | KD (nM) | kon (1/Ms) | Kdis (1/s) |
|---|---|---|---|
| **(1)** 100 | 0.76 | 4.99E+05 | 3.78E-04 |
| **(2)** 25 | 0.43 | 2.81E+05 | 1.22E-04 |

Figure S1. **Characterization of VHH-X118.** (A) VHH-X118 binds to CD8$^+$ cells. VHH-CTR, an irrelevant VHH used as control, does not stain CD8$^+$ cells, confirming the specificity of VHH-X118. (B) CD45$^+$ CD3$^+$ lymph node cells stained with antibodies to CD4, CD8α, CD8β, or VHH-X118 as indicated. VHH-X118 mean fluorescence intensity (MFI) decreased in the presence of anti-CD8α antibody (third panel) compared with the second panel but did not decrease in the presence of anti-CD8β antibody (fifth panel). (C) Dissociation constants for anti–mouse CD8 (VHH-X118) to mouse αβCD8 heterodimer were determined by biolayer interferometry (ForteBio Octet RED96 bio-layer interferometer) following the manufacturer's protocol.

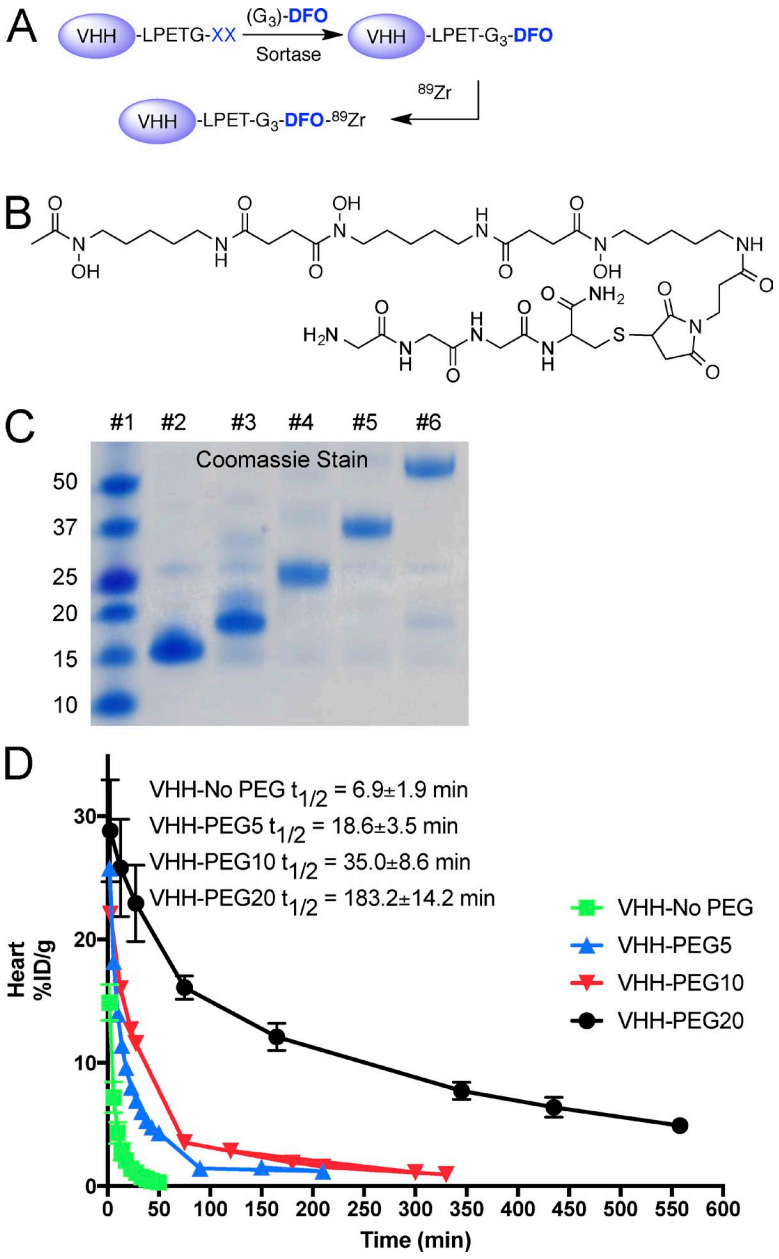


Figure S2. **Synthesis and characterization of modified VHH-X118.** (A) A sortase reaction was used to site-specifically label VHH-X118 with the desferroxiamine (DFO) chelator followed by $^{89}$Zr chelation. (B) Structure of $Gly_3$-DFO. (C) SDS-PAGE analysis shows installment of different size PEG molecules (5, 10, and 20 kD) onto VHH-X118 prelabeled with the biorthogonal substrate. Lanes are as follows: 1, marker; 2, VHH-X118; 3, azide-DFO–labeled VHH-X118 (VHH labeled with the biorthogonal substrate); 4, PEG5-VHH-X118; 5, PEG10-VHH-X118; and 6, PEG20-VHH-X118. (D) Circulatory half-life of non-PEGylated and PEGylated VHHs. Wild-type C57BL/6 mice were injected with 50 µCi $^{89}$Zr-labeled VHHs and imaged by PET at the indicated time points. Data were calculated as the percentage of injected dose per gram of blood in heart ($n$ = 3 for each measurement). Error bars represent standard deviation.

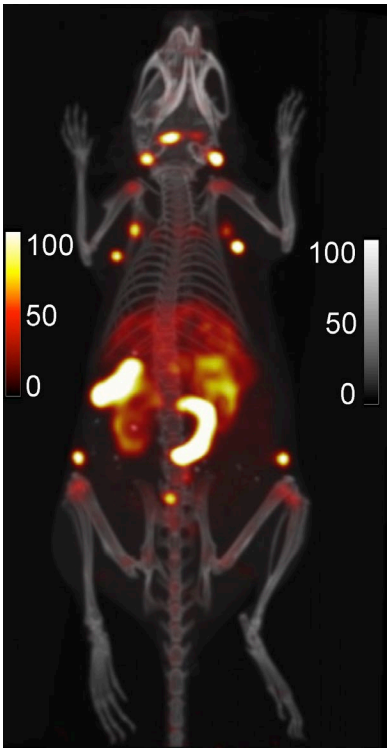


Figure S3. **A $^{89}$Zr-PEGylated VHH-X118 efficiently stains CD8$^{+}$ cells in lymphoid structures in OT-I RAGKO mice in vivo.** An enlarged mesenteric lymph node is a common feature of OT-I mice ($n$ = 2).

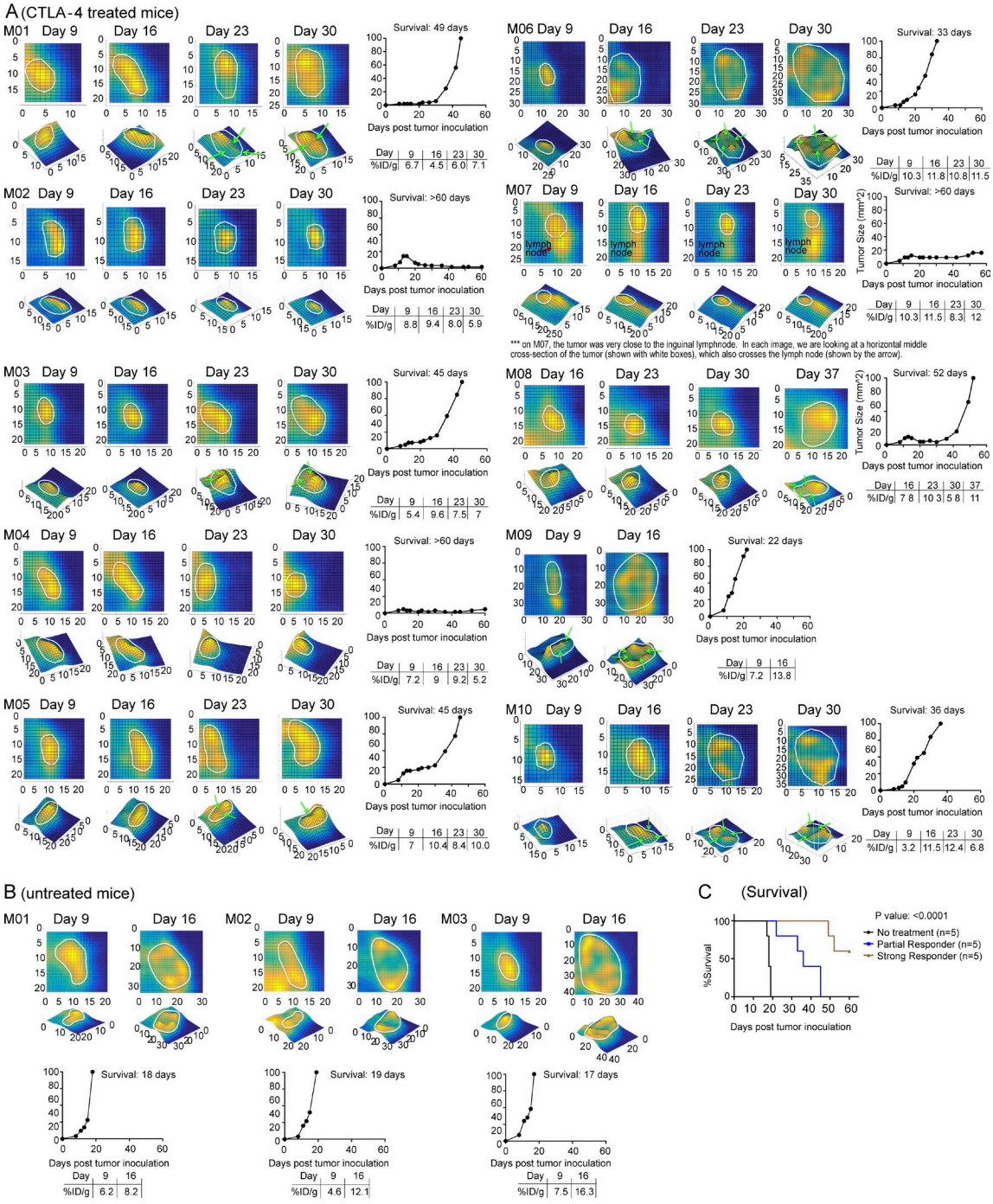


Figure S4. **Dynamics of CD8 T cell response and characterization of response patterns to immunotherapy and survival.** C57BL/6 mice were inoculated with B16 melanoma cells and GVAX simultaneously. Treatment with anti-CTLA4 (clone 9H10) started 1 wk after inoculation to obtain a heterogeneous antitumor response. Mice received CTLA4 therapy and were subjected to PET imaging according to the schedule shown in Fig. 4 A. (A) PET images of the tumors are shown in animals that received CTLA4 therapy. Tumors as identified by CT are outlined, and their size is indicated. The PET signals in the tumor are rendered as a heatmap. Below each image is the corresponding 3D graph, in which the z axis represents the strength of the PET signal (arbitrary units). The CD8 T cell signal was more homogenously distributed in mice with a strong response to CTLA4 treatment, whereas partial responders showed a more heterogeneous signal distribution. Where relevant, areas with lower PET signals are indicated by arrows. Each voxel is 0.42 × 0.42 mm. At right are graphs showing the growth of each tumor. Below the graphs are shown the percentage of injected dose per gram of tumors calculated based on PET images, normalized by muscle tissue. M01–M10 identify individual tumor-bearing CTLA-4–treated mice that were longitudinally imaged by X118 immunoPET. (B) Monitoring the response in untreated mice. M01–M3 identify individual tumor-bearing control mice. (C) Survival graph of mice in the different cohorts.

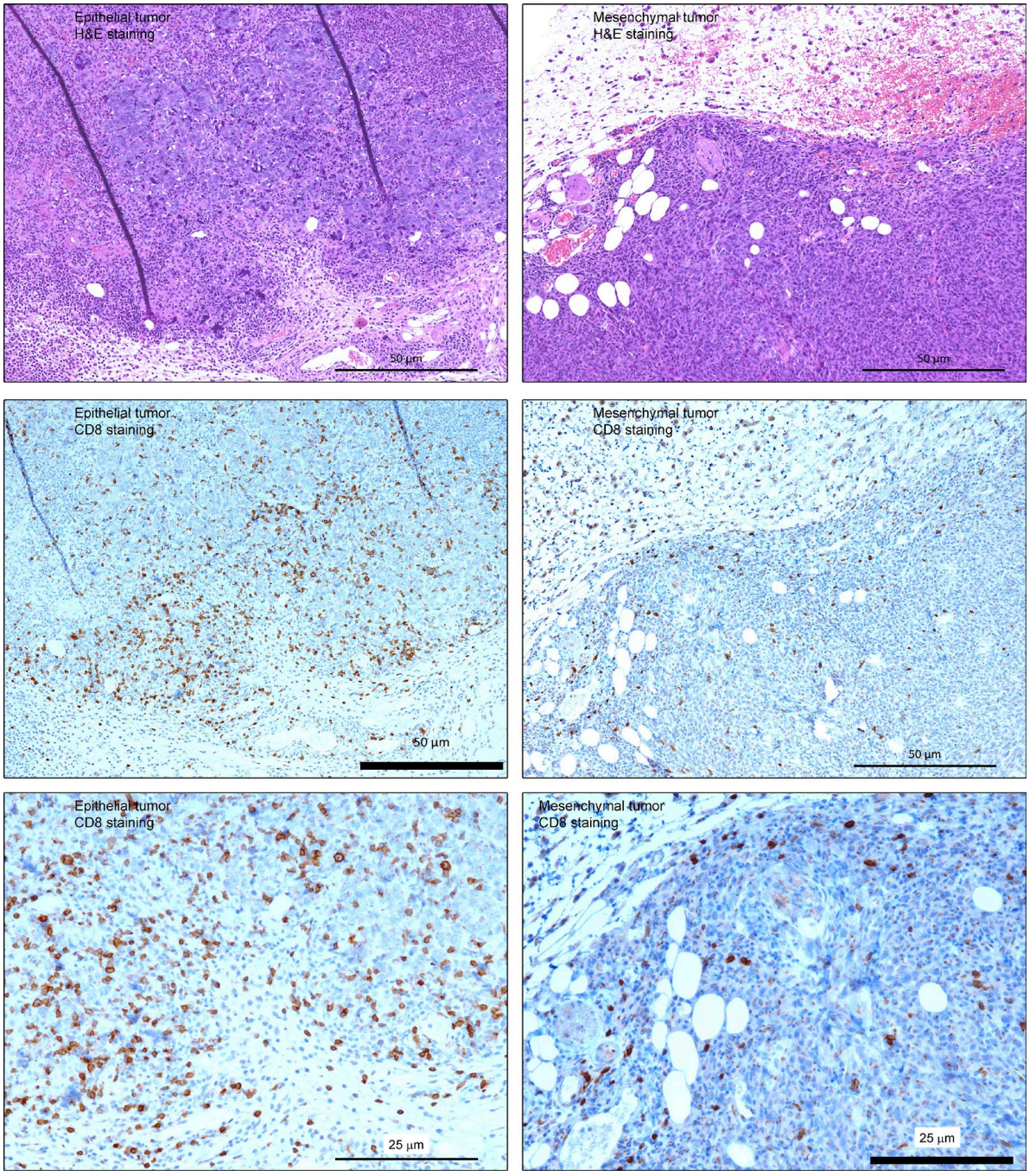


Figure S5. **H&E staining and immunohistochemistry ($CD8^+$ cells) of tumor samples ($n$ = 5 for each cohort).**

Video 1. **89Zr-VHH-X118 detects lymphoid organs.** Images were acquired 24 h p.i.

Video 2. **89Zr-PEG5-VHH-X118 detects lymphoid organs.** Images were acquired 24 h p.i.

Video 3. **89Zr-PEG10-VHH-X118 detects lymphoid organs.** Images were acquired 24 h p.i.

Video 4. **89Zr-PEG20-VHH-X118 detects lymphoid organs.** Images were acquired 24 h p.i.

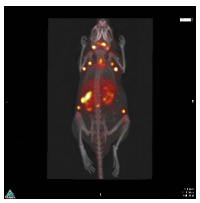

Video 5. **89Zr-PEG20-VHH-X118 detects lymphoid organs.** Images are acquired 48 h p.i.

Video 6. **89Zr-PEG20-VHH-X118 injected into a RAG-KO mouse.** No staining in lymphoid organs is observed. Images are acquired 24 h p.i.

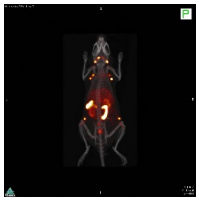

Video 7. **89Zr-PEG20-VHH-X118 detects lymphoid organs in OT1-RAGKO mouse.** Images were acquired 24 h p.i.

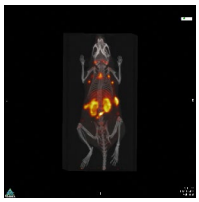

Video 8. **89Zr-PEG5-VHH-X118 detects lymphoid organs and the B16 tumor.** Images were acquired 24 h p.i.

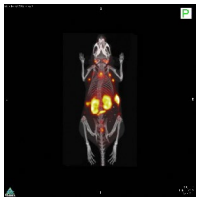

Video 9. **89Zr-PEG5-VHH-X118 detects lymphoid organs and the Panc02 tumor.** Images are acquired 24 h p.i.

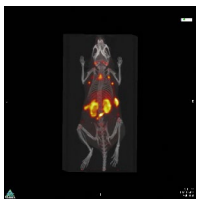

Video 10. **89Zr-PEG5-VHH-X118 detects lymphoid organs and the Panc02 tumor.** Images are acquired 48 h p.i.